JOURNAL OF MATERIALS SCIENCE 14 (1979) 2924–2928

Reaction sintering: correlation between densification and reaction

E. DI RUPO, M. R. ANSEAU*
Department of Materials Science, University of Mons, 15 Avenue Maistriau, 7000 Mons, Belgium

R. J. BROOK
Department of Ceramics, University of Leeds, Leeds, UK

By studying simultaneous densification kinetics and reaction kinetics during the sintering and hot pressing of alumina–zircon mixtures, it has been possible to distinguish between the particle rearrangement and particle reshaping (diffusive) stages of the densification process. Particle rearrangement is found to be more significant during hot pressing (20 MN m^{-2}) and is the dominant mechanism at relative densities up to 72%. In pressureless sintering, diffusive processes become dominant above relative densities of about 62%.

1. Introduction

A major problem in the analysis of densification kinetics has been that of separating the contributions to densification from different processes such as particle rearrangement, plastic flow, lattice diffusion, and grain boundary or second-phase diffusion. Although estimates of the relative importance of the different processes can be made for a given set of conditions by taking reasonable values for constants and by evaluating the different rate equations for the contributing processes (as in sintering maps [1]), these estimates are necessarily approximate in view of the geometrical assumptions made, the absence of comprehensive kinetic data (diffusion constants), and the sensitivity of available data to varying impurity levels.

As an alternative approach, it has been shown that an experimental discrimination between diffusive and non-diffusive contributions can be made [2] under the conditions of reaction hot-pressing, i.e. where densification and a chemical reaction are simultaneously occurring. It is the objective of the present work to apply this approach to the reactive sintering of the zircon–alumina system and, in particular, to compare the results with pressure sintering studies.

The basis for the approach has been discussed elsewhere [3, 2]. Briefly, it is founded on the use of the reaction rate to identify the diffusive contribution, the remaining contributions then being determined by the difference from the observed total densification rate. A requirement for its validity is that each diffusing atom contributes to both rates; this condition is most likely to hold in circumstances of densification by liquid phase or second phase assisted diffusion where solution–diffusion–reprecipitation sequences occur. The procedure has already been shown to apply well [4] in a study of the pressure dependence of the different contributions during the hot pressing of the zircon–alumina system.

2. Experimental

In terms of raw materials, hot-pressing procedure, and the analysis of reaction rate and density, the experimental methods have been described previously [4]. The additional method involved in the present study is that of pressureless sintering, and a brief account of that is therefore given below.

The zircon and alumina were added together in the ratio of two moles zircon (54.5 wt %) to three moles alumina (45.5 wt %); they were then mixed as powders with methyl alcohol for 12 h and dried.

* Centre de Recherche de l'Industrie Belge de la Céramique.

0022–2461/79/122924–05$02.50/0

About 100 g of the mixed powders were pressed with 2 wt % water as binder in a cylindrical die under a pressure of 1 MN m^{-2} for 2 min, and then dried at 110° C and pre-heated at 1000° C. The pre-heated samples were then placed in an electric furnace for different times at the chosen firing temperature (1400° C, 1450° C, 1500° C, 1550° C and 1600° C). At the end of the isotherms, the fired samples were taken out and placed in another electric furnace at 1000° C in order to prevent any thermal shock. The samples were then cooled down to room temperature for 5 h.

3. Results

The reaction between zircon and alumina follows the equation:

$$2ZrSiO_4 + 3Al_2O_3 \rightarrow 2ZrO_2 + 3Al_2O_3 \cdot 2SiO_2 \quad (1)$$

Quantities of zircon and alumina corresponding to this stoichiometric reaction were used in the preparation of all samples.

The results of the study of the temperature dependence of hot-pressing are given in Figs. 1 to 3 which show, respectively, the rates of densification for different temperatures, the complete compositional changes for the particular conditions of 20 MN m^{-2} applied pressure and 1550° C, and the temperature dependence of the reaction rate measured in terms of the residual alumina content. The densification rate is given as a continuous read-out; the reaction data are derived from analysis of samples rapidly cooled following treatment for the indicated times.

Similar data stemming from the sintering study are given in Figs. 4 to 6. Notable differences between the hot-pressing and pressureless sintering

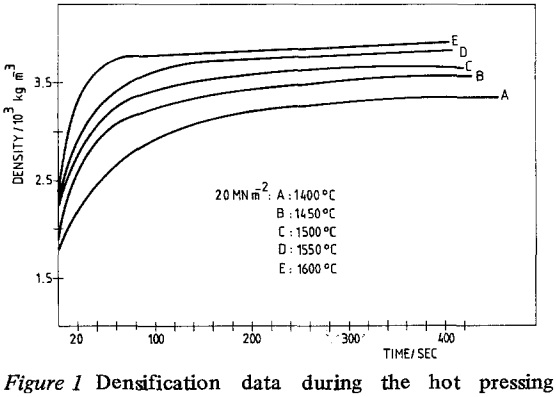

Figure 1 Densification data during the hot pressing (20 MN m^{-2}) of zircon–alumina mixtures.

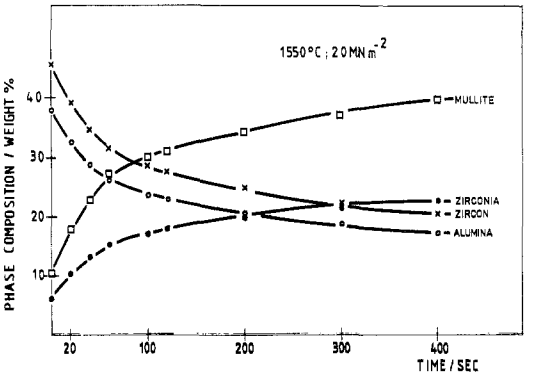

Figure 2 Progress of the chemical reaction during the hot-pressing of zircon–alumina mixtures.

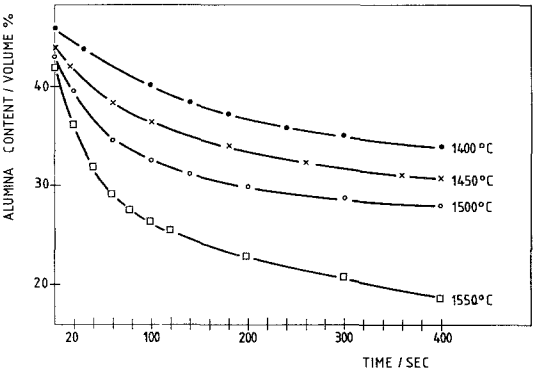

Figure 3 Temperature dependence of reaction rate during the hot-pressing of zircon–alumina mixtures. Assessment of the relative rates at constant alumina content shows an activation energy of 468 kJ mol^{-1}.

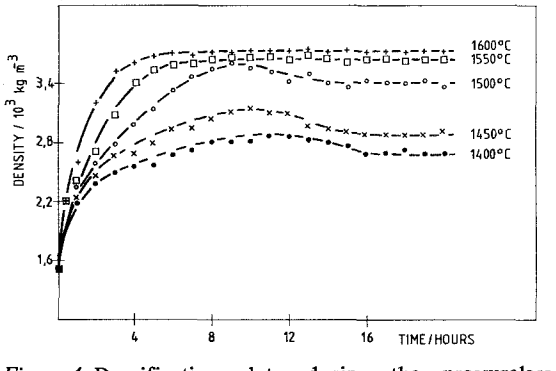

Figure 4 Densification data during the pressureless sintering of zircon–alumina mixtures. Assessment of the relative rates at constant density shows an activation energy of 439 kJ mol^{-1}.

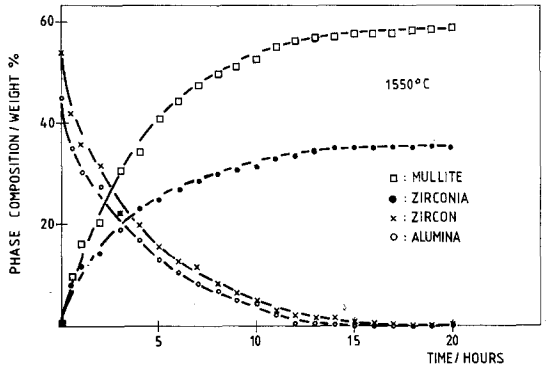

Figure 5 Progress of the chemical reaction during the sintering of zircon–alumina mixtures.

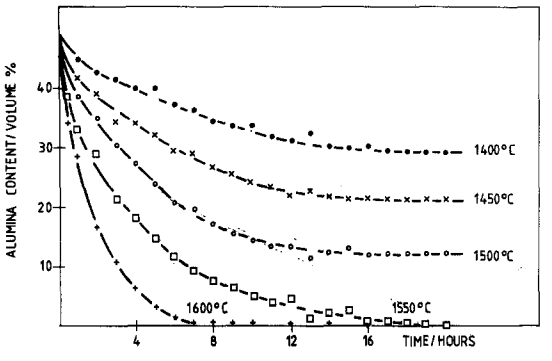

Figure 6 Temperature dependence of reaction rate during sintering of zircon–alumina mixtures. Assessment of relative rates at constant alumina content shows an activation energy of 318 kJ mol^{-1}.

results lie in the experimental times (typically minutes in hot-pressing and hours in pressureless sintering), and in the occurrence of a de-densification stage in the sintering runs at longer time. The latter is believed to result from partial disruption of high density specimens by continuation of the reaction.

4. Discussion

As argued in the earlier paper [4], the mechanisms for densification in this system are believed to consist of particle rearrangement (perhaps coupled with a degree of plastic deformation) and particle shape change resulting from diffusion of atoms through a boundary phase. The evidence for this argument lay in:

(a) a linear dependence of densification rate on applied pressure,

(b) a linear dependence of densification rate on the level of the alkali impurities believed to be responsible for the boundary phase, and

(c) a correlation between the sintering rate and the rate of chemical reaction that was consistent with the proposed mechanisms.

Following a similar pattern with the present data, the results are analysed by comparing the rates of densification and reaction at any point during processing. Then, by using the equation [3]

$$\left(\frac{1}{\rho}\frac{d\rho}{dt}\right)_{\text{diffusion}} = -\frac{2}{3}\left(\frac{1}{V}\frac{dV}{dt}\right) \qquad (2)$$

where ρ is the instantaneous density and V is the instantaneous amount of one of the reactants (in this study that of Al_2O_3), one can, from a knowledge of the reaction rate, estimate the fraction of densification arising from particle shape change by diffusion mechanisms. The particle rearrangement rate can then be evaluated from the argument

$$\left(\frac{1}{\rho}\frac{d\rho}{dt}\right)_{\text{total}} = \frac{1}{\rho}\left(\frac{d\rho}{dt}\right)_{\text{diffusion}} + \frac{1}{\rho}\left(\frac{d\rho}{dt}\right)_{\text{rearrangement}} \qquad (3)$$

This procedure was followed for the hot-pressing data in Fig. 7 where the reaction rate has been taken from the gradient of Fig. 3 and plotted against the densification rate taken from the gradient of Fig. 1. Each point represents data for a particular time, and the time direction is shown by the arrow, i.e. the shortest times at the right and the longer times at the left. The solid line represents the condition

$$\left(\frac{1}{\rho}\frac{d\rho}{dt}\right)_{\text{total}} = -\frac{2}{3}\left(\frac{1}{V}\frac{dV}{dt}\right) \qquad (4)$$

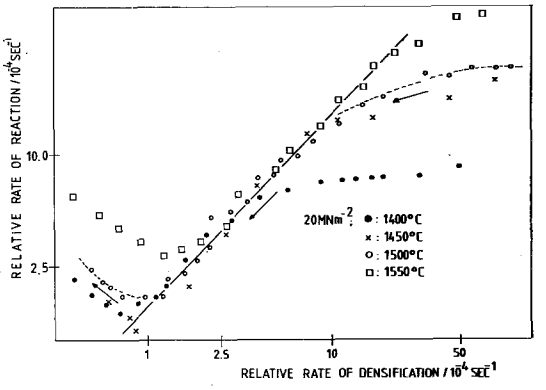

Figure 7 Comparison of reaction rate and densification rate for hot-pressed materials.

and is therefore valid when all densification is caused by the diffusion mechanism.

Fig. 7 shows, as in the earlier study of the pressure dependence [4] of hot-pressing, three stages: the first, where the densification is much more rapid than can be explained on the basis of diffusion, is believed to be attributable to particle rearrangement; the second, where data closely follow the theoretical line, corresponds to the diffusional mechanism as the dominant process; the third, where the reaction rate is more rapid than expected on the basis of the observed densification rate, is believed to correspond to continuing reaction in parts of the specimen where densification is complete, i.e. to reaction of grain cores.

The conditions of processing under which each mechanism (rearrangement, diffusion, core reaction) is dominant can be assessed by using Equation 3.

This is done for the temperature dependence of hot-pressing in Fig. 8; here the conditions of temperature and specimen relative density are shown corresponding to domination by one or other mechanism. It may be seen that the transition density from one process to another is essentially temperature independent; the relative density corresponding to the end of the rearrangement stage is approximately 72%.

In a similar way, data for pressureless sintering may be taken from Figs. 4 and 6; these are then compared in Fig. 9 from which the dominant mechanism can be abstracted as in Fig. 10. Two features that emerge clearly from comparing Figs. 10 and 8, i.e. pressureless sintering and hot-pressing, are first that the core reaction stage is less easy to distinguish during pressureless sintering, particularly at low temperature, and secondly, that the particle rearrangement process plays a much less important role in pressureless sintering. In this last respect, it may be seen that at densities greater than about 62%, diffusional processes have become dominant.

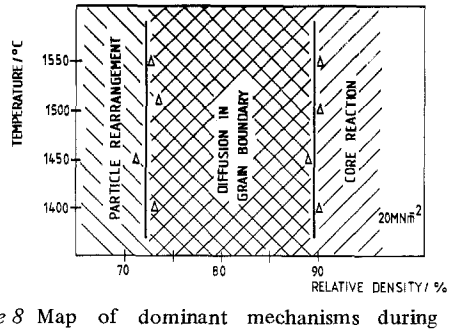

Figure 8 Map of dominant mechanisms during hot-pressing (20 MN m^{-2}).

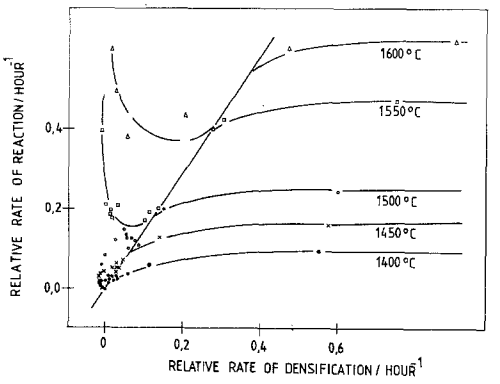

Figure 9 Comparison of reaction rate and densification rate for sintered materials.

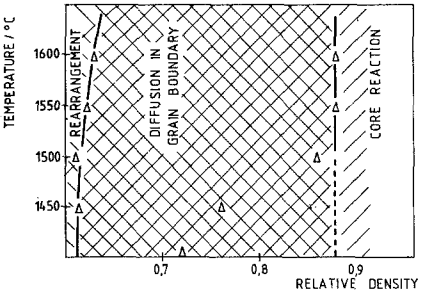

Figure 10 Map of dominant mechanisms during sintering.

5. Conclusions

The procedures for analysing densification data developed earlier for the hot-pressing of zircon–alumina ceramics [4] have been extended to the consideration of pressureless sintering data. It is found, as in the hot-pressing case, that the procedure allows the identification of the separate stages of densification and, in particular, that it shows the conditions under which diffusion processes are dominant.

A comparison of results from hot-pressing and from pressureless sintering shows clearly the greater contribution of diffusion processes to the latter. This is entirely consistent with the long-standing qualitative belief [5] that particle rearrangement processes are of greater importance in hot-pressing.

References

1. W. F. ASHBY, *Acta Met.* **20** (1971) 887.

2. E. DI RUPO, T. G. CARRUTHERS and R. J. BROOK, *J. Amer. Ceram. Soc.* **61** (1978) 468.
3. L. J. BOWEN, T. G. CARRUTHERS and R. J. BROOK, *ibid.* **61** (1978) 335.
4. E. DI RUPO, E. GILBART, T. G. CARRUTHERS and R. J. BROOK, *J. Mater. Sci.* **14** (1979) 705.
5. T. VASILOS and R. M. SPRIGGS, *Prog. Ceram. Sci.* **4** (1966) 95.

Received 11 April and accepted 26 July 1979.